Geometric and topological entropies of sphere packing

Jack A. Logan[1,2] and Alexei V. Tkachenko[2]
[1]*Department of Physics and Astronomy, Stony Brook University, Stony Brook, New York 11794, USA*
[2]*Center for Functional Nanomaterials, Brookhaven National Laboratory, Upton, New York 11973, USA*

(Received 26 March 2021; revised 23 September 2021; accepted 4 January 2022; published 18 January 2022)

We present a statistical mechanical description of randomly packed spherical particles, where the average coordination number is treated as a macroscopic thermodynamic variable. The overall packing entropy is shown to have two contributions: geometric, reflecting statistical weights of individual configurations, and topological, which corresponds to the number of topologically distinct states. Both of them are computed in the thermodynamic limit for isostatic and weakly underconstrained packings in 2D and 3D. The theory generalizes concepts of granular and glassy configurational entropies for the case of nonjammed systems. It is directly applicable to sticky colloids and predicts an asymptotic phase behavior of sticky spheres in the limit of strong binding.

DOI: 10.1103/PhysRevE.105.014117

I. INTRODUCTION

The deceivingly simple task of packing spheres has been an inspiration for multiple problems in mathematics and natural sciences since the times of Kepler [1]. It provides insights into the physics of crystalline solids, as well as into the world of disordered states of matter [2–4]. One such fundamental problem is finding the entropy of a random packing of spheres. In its simplified form, this amounts to counting the number of ways in which distinct particle arrangements can be generated for a given ensemble. For instance, more than two decades ago, Sam Edwards introduced the notion of granular entropy [5,6]. A similar concept also arises in the context of hard-sphere glasses as a measure of degeneracy of the locally stable configurations [4,7]. In both examples, the packing entropy would be a measure of the multiplicity of the jammed states. Due to the nonequilibrium nature of jamming, even a rigorous definition of the granular entropy remains nontrivial. Nevertheless, significant progress in understanding and computing it has been demonstrated in recent years [8–11].

In this paper, we discuss the packing entropy in an equilibrium system of spheres, where it can be properly defined as a conventional thermodynamic quantity. The system studied is not jammed but rather is constrained to have a specific number of direct interparticle contacts. In other words, we use the total number of contacts (or, equivalently, mean coordination number of the particles, Z) as a thermodynamic variable. This approach is immediately relevant to packings of sticky spheres where each contact is associated with a fixed binding energy. Two limits of that problem have been explored in the past: thermodynamics of a sticky sphere liquid (e.g., Baxter model) [12,13] and, more recently, free-energy landscapes and kinetics of mesoscopic multicolloidal clusters [14–19]. In this paper, we seek to bridge the gap between these two limits and, more importantly, use this model system to better understand the nature of packing entropy. The latter can be subsequently connected to the granular and/or glassy entropy by applying external pressure to the system that would lead to its jamming. The difference from the original contexts in which those entropies were introduced is that one would start with an already discrete configurational space and select its subset that corresponds to the local minima of the total volume.

II. PARTITIONING OF PACKING ENTROPY

Consider a system of N hard spherical particles in d-dimensional space, with average particle diameter $\bar{a}$. The packing is weakly polydisperse, so the width of the particle diameter distribution is much smaller than the average: $\delta a \ll \bar{a}$. We define a pair of particles to be in contact if the gap between them is less than some small value $\Delta \ll \bar{a}$. The gap between particles i and j is defined as $x_{ij} = |\mathbf{r}_i - \mathbf{r}_j| - (a_i + a_j)/2$, where a and $\mathbf{r}$ are their respective diameters and positions. For any configuration, the topology of the packing can be specified by an adjacency matrix $\hat{\mathbf{C}}$, with elements $C_{ij} = 1$ for all particles $i \neq j$ in contact, and $C_{ij} = 0$ otherwise. As already mentioned above, the average coordination number $Z = 1/N \sum_{i<j} C_{ij}$ is treated as a macroscopic thermodynamic variable of the system. Note that throughout the paper, we set $k_B T = 1$.

The weak polydispersity is introduced to avoid hyperstatic (overconstrained) configurations. These contain accidental contacts that could be removed, e.g., by slight variations of particle sizes (subject to the constraint that all other contacts are intact). Examples of such overconstrained configurations are close packed crystals (face-centered cubic (FCC)/hexagonal close-packed (HCP) in 3D or hexagonal lattice in 2D). If those are disqualified, any rigid packing has to be isostatic, i.e., the number of contacts has to be equal to the total number of degrees of freedom of N spheres, dN, minus the number of rigid body degrees of freedom of the packing as a whole, $d(d+1)/2$ [20,21]. In the thermodynamic

limit, this corresponds to $Z^* = 2d$, while for a finite isostatic packing $Z^* = 2d - d(d+1)/N$. Below we start by discussing the isostatic limit, and then generalize our results to the underconstrained case $Z < Z^*$, in which each missing bond gives rise to a single zero mode.

The *packing entropy* for a given Z is found by performing the summation of statistical weights of all topologically distinct realizations:

$$e^{NS_{\rm pack}(Z)} = \sum_{\hat{\mathbf{C}}} \frac{\delta(Z(\hat{\mathbf{C}}) - Z)}{N!} e^{NS_{\rm geo}(\hat{\mathbf{C}})} \tag{1}$$

Here we have introduced the *geometric entropy* $S_{\rm geo}(\hat{\mathbf{C}})$ which determines the statistical weight of a specific realization of the packing:

$$e^{NS_{\rm geo}(\hat{\mathbf{C}})} = \int \frac{d^d\mathbf{r}_2 \ldots d^d\mathbf{r}_N}{\Omega_d \bar{a}^{(N-1)d}} \prod_{i>j, C_{ij}=1} \bar{a}\delta(x_{ij}) \prod_{i>j, C_{ij}=0} \Theta(x_{ij}). \tag{2}$$

This expression assumes that all N spheres belong to a single cluster. The statistical weight is determined up to a constant factor, and here we use dimensions of average particle diameter $\bar{a}$. Division by the factor Ω_d eliminates contributions from its rigid body rotations (specifically, $\Omega_2 = 2\pi$ for 2D and $\Omega_3 = 2\pi \times 4\pi = 8\pi^2$ for 3D). Translation of the cluster as a whole is not included since integration is only performed over positions of $N-1$ out of N spheres. Without loss of generality, the position of the first particle $\mathbf{r}_1$ will be assumed to be fixed at the origin. The factor $N!$ in Eq. (1) deserves special clarification due to the widespread confusion regarding its origin in statistical mechanics. As we show in Appendix A, this factor does not require the particles to be indistinguishable and, moreover, it has nothing to do with quantum mechanics [10,18].

III. ISOSTATIC PACKING

A. Geometric entropy of isostatic packings

For an isostatic packing, we can switch variables from the positions $(\mathbf{r}_2, \ldots, \mathbf{r}_N)$ to the gaps between pairs of particles in contact, $(x_1, \ldots, x_{NZ/2})$. The new variables should also include $d(d-1)/2$ independent rigid body rotations of the cluster: $\hat{\theta} = (\theta_1 \ldots, \theta_{d(d-1)/2})$. The Jacobian associated with this change in variables is known as the rigidity matrix [15]. According to Eq. (2), the corresponding Jacobian determinant can be used to find the geometric entropy:

$$NS_{\rm geo}(\hat{\mathbf{C}}) = \ln\left[\frac{\partial(\mathbf{r}_2, \ldots, \mathbf{r}_N)}{\partial(\hat{\theta}, x_1, \ldots, x_{NZ/2})}\right]. \tag{3}$$

While this equation can be used to find the geometric entropy of any isostatic configuration, when using it to find the statistical weight for hard spheres we must exclude any configurations that lead to overlaps between particles.

A more conventional approach to finding the statistical weight for each topologically distinct configuration, e.g., in the context of sticky colloids, is to calculate the free energy that includes both phonons and rigid body modes of the entire packing [14–18]. That route is practical but it has led to a number of seemingly paradoxical observations. In particular, one needs to assign specific masses to all the particles and replace rigid bonds with effective springs. Of course, in the nonquantum regime, masses may only give a constant contribution to the free energy. And yet, the overall statistical weight of a cluster in this formulation depends, e.g., on its moment of inertia [18]. The paradox may be resolved by the direct demonstration that when the phonon and rotational partition functions are combined, all of the masses would only give rise to a trivial multiplier, independent of specific configurations [19]. The same is true for the spring constants: As expected in the isostatic case, the free energy is not sensitive to the details of the bonding potential [17]. The geometric entropy gives the statistical weights of any configuration in the form of Eq. (3), making the phonon-based calculation redundant.

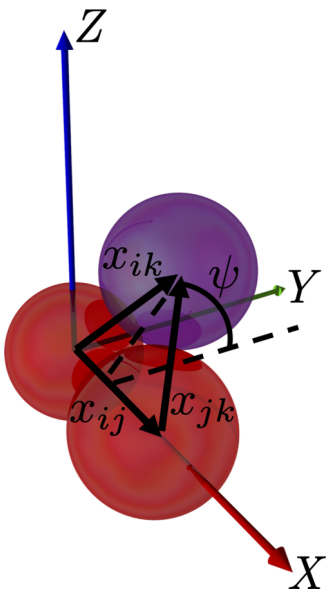

FIG. 1. Minimal cluster in 3D. Initial two particles (i and j) shown in red along the X axis in contact with particle k (purple). Particle k has a rotational degree of freedom, here seen at an angle ψ with the XY plane, that allows it to remain in contact with the other particles.

Below we present several examples of calculating the geometric entropy. The first case is a minimal cluster, defined as d spherical particles in d dimensions, all in contact with each other, such as the one shown in Fig. 1. Let us demonstrate that $S_{\rm geo} = 0$ for a minimal cluster. Consider two identical particles, i and j, of diameter a. Particle i is fixed as the origin of the system and particle j is placed along the X axis in contact with i, as shown in Fig. 1. To get the Jacobian, we consider infinitesimal displacements $\delta\mathbf{r}$, $\delta\boldsymbol{\theta}$, $\delta\boldsymbol{\phi}$. The effect of $\delta\mathbf{r}$ is to change the gap x_{ij} between the particles, while the other two displacements lead to small changes in y_j and z_j through infinitesimal rotations. Altogether, we find

$$\begin{bmatrix} \delta x_j \\ \delta y_j \\ \delta z_j \end{bmatrix} = \begin{bmatrix} 1 & 0 & 0 \\ 0 & a & 0 \\ 0 & 0 & -a \end{bmatrix} \begin{bmatrix} \delta r \\ \delta\theta \\ \delta\phi \end{bmatrix}. \tag{4}$$

The Jacobian determinant, given $a = 1$, is then $|J| = 1$. This serves two purposes: it allows us to build to a 3D minimal

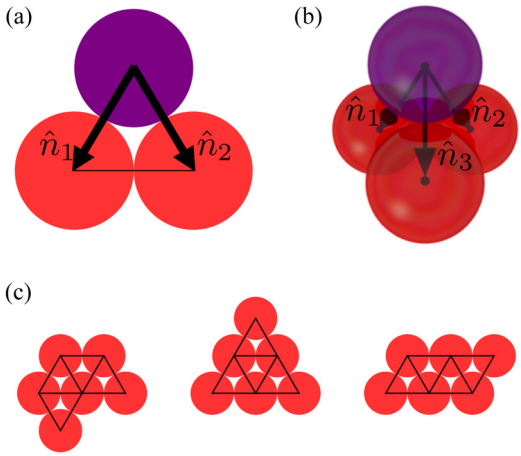

FIG. 2. (a), (b) Minimal clusters (red) for $d = 2$ and $d = 3$. An additional particle (purple) bonds to each particle in the minimal cluster along vectors $\hat{n}_i$. (c) Three six-particle clusters with the same S_{geo}, despite having different topologies.

cluster one particle at a time, and restricting above to the XY plane shows that a 2D minimal cluster has geometric entropy of zero.

For a minimal cluster in 3D, we add a third identical particle k to the configuration above. The two previous particles are fixed along the X axis and the third particle is placed in contact with them. We need to transform coordinates from (x_k, y_k, z_k) to (x_{ik}, x_{jk}, ψ), where ψ is the angle from the XY plane to particle k, and x_{ik} and x_{jk} are the gaps between the particles. Again we consider infinitesimal displacements, this time in $\delta\mathbf{x_k}$, $\delta\mathbf{y_k}$, and $\delta\mathbf{z_k}$ and write down how it affects the gap sizes x_{ik}, x_{jk}, and the tilt angle ψ:

$$\begin{bmatrix} \delta x_{ik} \\ \delta x_{jk} \\ \delta\psi \end{bmatrix} = \begin{bmatrix} \frac{1}{2} & 0 & \frac{\sqrt{3}}{2} \\ -\frac{1}{2} & 0 & \frac{\sqrt{3}}{2} \\ 0 & -\frac{2}{\sqrt{3}} & 0 \end{bmatrix} \begin{bmatrix} \delta x_k \\ \delta y_k \\ \delta z_k \end{bmatrix}. \tag{5}$$

We find the Jacobian determinant is again $|J| = 1$. For 3D, the product of the Jacobians for each individual particle gives the complete Jacobian value. The entropy is then found as the natural logarithm of the Jacobian, $S_{\text{geo}} = \ln(1) = 0$.

The next most trivial cluster is formed by adding a particle that bonds to each of the particles in the minimal cluster, such as the purple particles shown in Fig. 2. In 2D, the geometric entropy associated with this additional particle is $S_{\text{geo}} = \ln[\hat{n}_1 \times \hat{n}_2]$, where $\hat{n}_i$ are unit vectors in the directions of the bonds. If the particles are arranged in a square lattice, for example, the bond directions $\hat{n}_1$ and $\hat{n}_2$ are orthogonal, and hence $S_{\text{geo}} = 0$. In the case of a triangular lattice, however, each additional particle forms an equilateral triangle and adds $-\ln(\frac{\sqrt{3}}{2})$ to the overall geometric entropy of the minimal cluster. Similarly in 3D, adding a particle to the minimal cluster creates a regular tetrahedron and the triple product of the unit vectors along the bonds adds $-\ln(\frac{1}{\sqrt{2}})$ to the geometric entropy. Just like the square lattice in 2D, a cubic lattice is a special case of an isostatic packing with $S_{\text{geo}} = 0$ because the bonds are mutually orthogonal.

We can continue to add particles to the minimal clusters that have exactly d bonds each, maintaining the isostaticity of the packing. Three such examples where four particles have been added to a 2D minimal cluster are shown in Fig. 2(c). The addition of each new particle always increases the cumulative geometric entropy of the cluster by $-\ln(\frac{\sqrt{3}}{2})$. For this reason, despite the differences in their topologies, they all have the same S_{geo}. Note, however, that if the distinction between particles is ignored, the higher-symmetry triangular cluster would have a *lower* statistical weight, as it corresponds to a smaller number of nontrivial particle permutations [16,19].

B. Topological entropy of isostatic packings

The overall packing entropy can be expressed as

$$S_{\text{pack}} = \langle S_{\text{geo}} \rangle + S_{\text{topo}}. \tag{6}$$

Here $\langle ... \rangle$ denotes the averaging over all topological realizations, weighted proportionally to $\exp(NS_{\text{geo}})$, for a given coordination number Z (e.g., $Z = Z^*$ for the currently discussed isostatic case). The topological entropy S_{topo} is an analog of Edwards entropy: It has the interpretation as the logarithm of the number of distinct realizations. The fact that $-NS_{\text{geo}}$ acts as an effective Hamiltonian enables one to employ a Monte Carlo (MC) approach to generate the equilibrium ensemble of isostatic packs and calculate, e.g., $\langle S_{\text{geo}} \rangle$ itself or any other ensemble-averaged quantity. However, the generated energy landscape is very rough, with lots of local minima, and making large, nonlocal moves to escape them is highly nontrivial. To resolve this complication, we introduce a generalized effective Hamiltonian, $H_{\text{eff}} = -\lambda N S_{\text{geo}}(\hat{\mathbf{C}})$. The parameter λ here allows one to tune the model from its original form (for $\lambda = 1$) to one with a completely flat energy landscape (in $\lambda = 0$ limit). That limit corresponds to a model in which all plausible topological arrangements with the same coordination number Z have the same statistical weight. MC simulations are run for $\lambda = 0$ and the results for $\lambda = 1$ are extrapolated from those simulations by calculating the response to field λ.

Let $S^{(0)}_{\text{geo}} = \langle S_{\text{geo}} \rangle$ and $S^{(0)}_{\text{pack}}$ be the geometric and full packing entropies computed for $\lambda = 0$ [note that topological entropy in the limit $\lambda = 0$ is identical to $S^{(0)}_{\text{pack}}$]. By expressing S_{topo} in the vicinity of its maximum value for $\lambda = 0$, in terms of $s \equiv S_{\text{geo}} - S^{(0)}_{\text{geo}}$, we obtain the following Landau-style expansion:

$$\begin{aligned} S_{\text{pack}}(\lambda, s) &= S_{\text{topo}}(s) + \lambda\big(S^{(0)}_{\text{geo}} + s\big) \\ &= S^{(0)}_{\text{pack}} + \lambda\big(S^{(0)}_{\text{geo}} + s\big) - \frac{s^2}{2\chi} + \frac{s^3}{6\chi'} + \cdots \end{aligned} \tag{7}$$

Here we used the fact that, by definition, the distribution function $f(s) \sim e^{NS_{\text{pack}}(\lambda, s)}$. Therefore, the coefficients in this expansion can be extracted from the statistics of S_{geo} computed at $\lambda = 0$. For instance, $\chi = N\langle s^2 \rangle$. By maximizing Eq. (7) with respect to s, one can extrapolate geometric, topological, and the overall packing entropy to $\lambda = 1$. In leading order, that gives $S_{\text{geo}} \approx S^{(0)}_{\text{geo}} + \chi$ and $S_{\text{topo}} = S^{(0)}_{\text{pack}} - \frac{\chi}{2}$. As demonstrated in Appendix B, accounting for higher-order terms in Eq. (7) yields only a slight correction to these results.

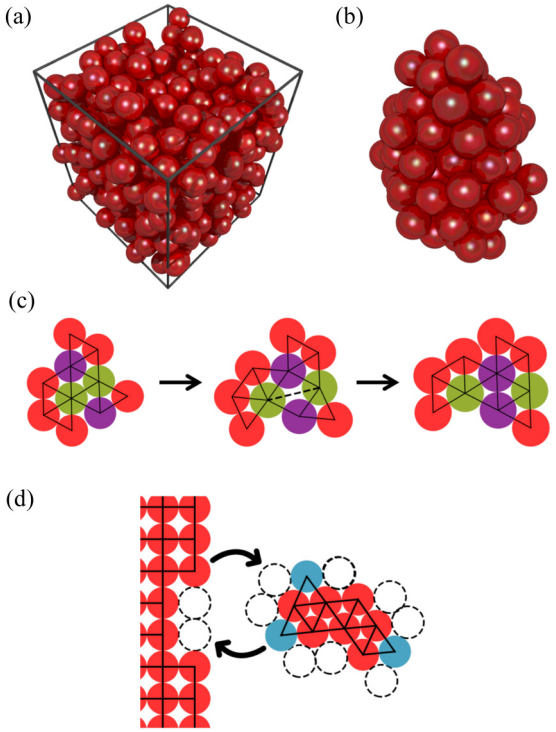

FIG. 3. Example packings. (a) Packing with periodic boundary conditions in the horizontal directions, with a closed bottom but open upward. (b) A typical cluster packing in free space. (c) A typical Monte Carlo move. The bonded green particles slowly open, allowing the packing to move along a single zero mode until the purple particles make contact. At this point, the bond is broken between the green pair of particles and created between the purple particles, completing the move to a new topological state. (d) A cluster packing in equilibrium with an infinitely large square lattice. At any moment, a free particle may condense onto the packing in any of the N_+ positions where it will have exactly d bonds (dashed open circles). Likewise, any of the N_- particles in the packing with exactly d bonds (blue) may evaporate off the packing and back to the lattice. Here $N_+ = 9$ (the top center particle in fact represents two particles, closely spaced) and $N_- = 3$.

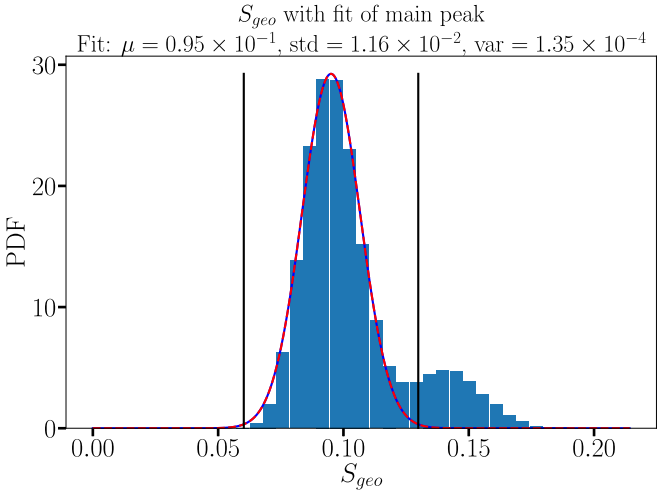

FIG. 4. The original S_{geo} probability density function (PDF) for the 400-particle PBC packings. A clear second peak is seen that points to zero modes persisting in the configurations after a new topology is made. Fit with a normal distribution in dashed red. The black vertical lines represent 3σ of the fit.

Below we describe the numerical procedure that was used to compute $S^{(0)}_{\text{geo}}$, χ and $S^{(0)}_{\text{pack}}$.

IV. MONTE CARLO SIMULATION

A. Isostaticity-preserving MC move

In our simulations, it was ensured that the packing remains strictly isostatic and does not have any interparticle overlaps. A typical MC move is illustrated in Fig. 3(c): A randomly chosen bond is broken, and the gap between the two particles increases, while all the spheres are pushed along the single zero mode associated with the lost contact. The move is complete once two, previously unbound, particles make contact. If $\lambda = 0$, there is no difference in statistical weights between different (isostatic) configurations, so the only constraint is nonoverlapping of the particles.

Two different classes of isostatic systems have been studied: (i) packings in a semiperiodic box with periodic boundary conditions (PBCs) along the x and y axes and a free boundary in the upward z direction (only x and z axes in 2D) and (ii) clusters in open space. In both cases, the size of the system was gradually increased by adding one particle at a time in a way that preserved the overall isostaticity. Examples of both packing types can be seen in Figs. 3(a) and 3(b).

A packing, whether PBC or cluster, evolves in a dN-dimensional space that can be represented by the positions of the N spheres or the dN bond gaps. The constraints for them to be hard spheres in contact are given by $|\vec{r}_i - \vec{r}_j|^2 = (\frac{a_i+a_j}{2})^2$. The Jacobian of this equation is the rigidity tensor, shown in Eq. (3). At each step of our simulations, a bond is broken and a zero mode enters into the packing. The packing then evolves in such a way that it moves orthogonal to the constraints imposed by the rigidity tensor until contact is made between two unbonded particles and a new isostatic packing is realized. The rigidity tensor $R(\vec{r})$ relates the particle displacements $\vec{u}_i$ to the gaps between particles x_{ij}. If we consider that the bond α breaks and opens by an amount x_α, the displacement of any particle i can be calculated as $\vec{u}_i = R^{-1}_{i,\alpha} x_\alpha$. However, to avoid the computationally expensive inverse function, we instead use a QR decomposition with column pivoting [22] to solve the equation for the displacements $\vec{u}_i$ of all particles caused by the opening of α. By using Eq. (3), the distribution of S_{geo} has been computed directly, which determines the parameters $S^{(0)}_{\text{geo}}$ and χ in Eq. (7).

It's important that the trajectory of the evolution moves the packing from one isostatic configuration to another. The new bond that should be made is completely determined by the specific bond that is broken. Sometimes, however, due to the finite precision of the simulation, a bond other than the true bond will close. When this occurs, one part of the packing will be overconstrained, while a zero mode will persist in another. This zero mode appears as an anomalously high geometric entropy in our distribution, as demonstrated by the second peak that appears at larger values than the main peak in Fig. 4. This peak is a collection of packings that were made when

the incorrect bond was closed. To maintain results that only include true isostatic packings, we must filter out the configurations that include zero modes. We first fit our main peak with a normal distribution, shown in red in the figure. The black vertical lines mark three standard deviations from the mean of the fit. Any data outside the black lines is assumed to come from a zero mode configuration and is discarded.

B. Virtual exchange with reference packing

To compute $S^{(0)}_{\text{pack}}$, we imagine that the packing can exchange particles with an infinitely large cubic (or square in 2D) lattice through evaporation and condensation events, as shown in Fig. 3(d). Technically, particles have not been moved between the random packing and the reference lattice, but only the probabilities of such moves have been computed. In equilibrium, the chemical potential of particles in the random packing, $\mu = -S^{(0)}_{\text{pack}}$, should match that in the reference lattice. For any configuration, we find a number N_+ of sites where a particle can be added to the packing and a number N_- of removable particles that have exactly d bonds. By requiring the addition and removal processes to balance each other, one obtains $S^{(0)}_{\text{pack}} = -\mu = \ln(\langle N_+\rangle/\langle N_-\rangle)$.

We begin a PBC simulation with a fixed layer of particles at the base of the box ($z = 0$). This layer acts as a substrate on which particles can adsorb. These substrate particles are fixed throughout the simulation but any bonds they share with free particles are not. For the packing to be isostatic, it requires dN_{free} bonds to match the number of translational degrees of freedom from the free particles. We use Eq. (3) to calculate the geometric entropy for each configuration.

To build a packing, we first identify every possible location where a new particle could come into existence and have exactly d bonds without leading to any overlaps with the current particles. We call these positions virtual particles. In general, for any configuration there exists an enormous number of virtual particles and we randomly choose one in a way that tends to maximize our packing fraction by applying a weight to each virtual particle. While building the packing to the desired number of particles, our MC move [Fig. 3(c)] is used to rearrange the packing, allowing it to mix while it grows. The results are not particularly meaningful while the number of particles is constantly changing, so no data is collected while a packing is growing.

V. RESULTS

A. Entropies of isostatic packings

Our results for the topological and geometric entropies are shown in Fig. 5 as functions of packing size for both cases of PBCs and clusters. Note the excellent agreement between the two methods, and that the entropies appear consistent across all N. The implied infinite-size values of different types of entropies for 2D and 3D are presented in Table I. Interestingly, the obtained geometric entropies are quite close to our original estimates, which were based on a sequential packing procedure: $S_{\text{geo}} \approx 0.15 \pm 0.01$ vs $-\ln(\frac{\sqrt{3}}{2}) \approx 0.14$ in 2D, and $S_{\text{geo}} \approx 0.35 \pm 0.04$ vs $-\ln(\frac{1}{\sqrt{2}}) \approx 0.35$ in 3D. Topological entropies in both cases are quite substantial: 1.52 ± 0.13 and 3.02 ± 0.32, respectively. It is important to keep in mind that we are exploring the space of isostatic packs rather than jammed ones. In other words, they do not represent local density maxima. This explains why our results for the topological entropy are significantly larger than those extracted from recent computations of granular entropies: 0.5 and 0.7 for 2D and 3D, respectively [10,11]. This also explains why the observed equilibrium volume fraction in 3D is significantly lower than that of random close packing (or maximally random jammed state defined in Ref. [3]). For 3D, PBC packings show a value of $\eta \approx 0.52$, which is close to the density of a cubic lattice, and cluster packings are somewhat higher at $\eta \approx 0.56$. Curiously, the found equilibrium value $\eta_0 \approx 0.54 \pm 0.02$ is close to the so-called random loose packing density [23], although this is likely to be just a coincidence.

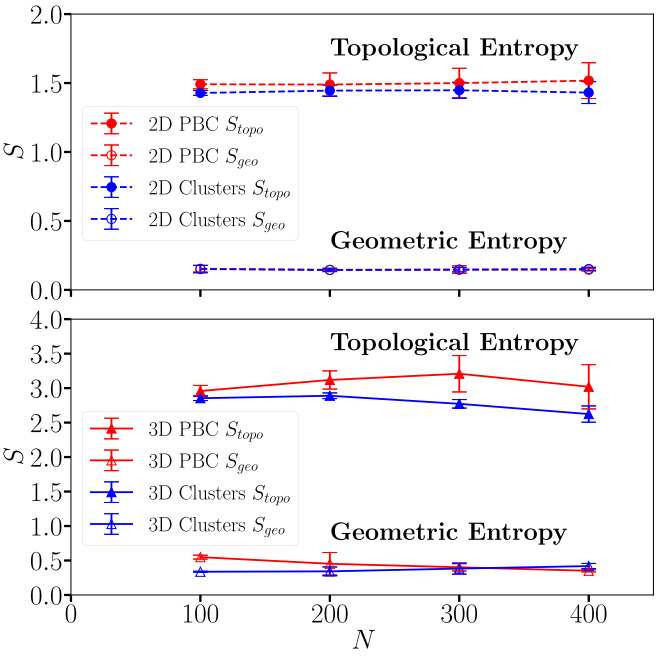

FIG. 5. Geometric and topological entropy values per particle for 2D (top, dashed) and 3D (bottom, solid), including PBC and cluster packings with the number of particles in a packing N up to 400.

B. Geometric and topological entropies of underconstrained packings

In our paper, we primarily focused on the isostatic case, where the number of contacts exactly matched the number of

TABLE I. The geometric, topological, and full packing entropy per particle in 2D and 3D Cluster and PBC packings with 400 particles.

		PBC	Clusters
$d = 2$	S_{pack}	1.66	1.58
	S_{geo}	0.15	0.15
	S_{topo}	1.52	1.43
$d = 3$	S_{pack}	3.37	3.04
	S_{geo}	0.35	0.42
	S_{topo}	3.02	2.62

frozen degrees of freedom in a rigid packing. To expand our approach to the underconstrained case of so-called floppy networks, we note that breaking any bond in an isostatic network generates a single zero mode. Such a mode is bounded by two isostatic states. This allows one to count the number of distinct configurations with exactly one zero mode: $e^{NS_{\rm topo}(Z^*)}N_c/2$. Here $e^{S_{\rm topo}(Z^*)}$ is the number of distinct isostatic arrangements, $N_c^* = NZ^*/2$ is the number of bonds in an isostatic state, and the factor of $1/2$ accounts for double counting. This bond-breaking procedure can be repeated again to generate an ensemble of all floppy networks with $M_0 = N(Z^* - Z)/2$ zero modes. As long as $M_0 \ll N_c^*$, one may ignore the order in which the bonds in the original isostatic packing had been broken. Hence, for each of those packings, the number of unique floppy networks generated is $\frac{N_c^*!2^{-M_c}}{(N_c^*-M_0)!M_0!}$. After using Stirling approximation, we obtain the following result for the topological entropy:

$$S_{\rm topo}(Z) \approx S_{\rm topo}(Z^*) + \frac{Z^* - Z}{2}\ln\left[\frac{Z^*}{2(Z^* - Z)}\right]. \quad (8)$$

As for the geometric entropy, it is obtained by integration over all activated zero modes and the corresponding correction is simply proportional to their number:

$$S_{\rm geo}(Z) \approx S_{\rm geo}(Z^*) + \frac{Z^* - Z}{2}\ln(\xi/\bar{a}). \quad (9)$$

Here ξ represents the typical range over which the interparticle gap x_{ij} may change until the new contact is formed.

In the specific case of sticky spheres, the packing entropy $S_{\rm topo} + S_{\rm geo}$ makes an important contribution to the chemical potential of a disordered aggregate (i.e., a large cluster):

$$\mu(Z) = \frac{\epsilon Z}{2} - S_{\rm geo}(Z) - S_{\rm topo}(Z). \quad (10)$$

Here $\epsilon = \ln(12\tau)$ is the binding free energy. Minimization of the chemical potential $\mu(Z)$ predicts an exponential suppression of zero modes with bond strength: $(Z^* - Z) \sim e^{-\epsilon}$. Therefore, residual topological and geometric entropies of an aggregate are close to their isostatic values, given in Table I.

C. Application to sticky spheres

The obtained results can be naturally applied to sticky colloids by assigning binding free energy $\epsilon = \ln(12\tau)$ to each interparticle bond. Here τ is introduced for consistency with the widely used Baxter model [12,13], where this parameter is known as the Baxter temperature. In fact, our results can be applied for an arbitrary short-range potential $V(r)$ by setting $12\tau = 1/(\int_0^\infty \exp(-V(x))dx/\bar{a})$. According to the Baxter model, the dense and dilute fluid phases coexist below the critical point $\tau_c \approx 0.1$. Historically, most of the numerical and analytic studies have been focused on the regime of modest attraction, $\tau \simeq \tau_c$. Our approach provides a complementary description in the strong binding limit, $\tau \ll \tau_c$.

In this case, the dilute phase can be well described as an ideal gas. In contrast, the dense liquid phase is nearly isostatic, since each broken bond is associated with a substantial free-energy penalty. This leads to a simple result for μ and hence for the density of the dilute phase $\rho \equiv N\bar{a}^d/V = 6\eta/\pi$ as a function of τ:

$$\mu = \frac{Z^*}{2}\ln(12\tau) - S_{\rm pack}, \quad (11)$$

$$\rho(\tau) = e^{\mu} = (12\tau)^d e^{-S_{\rm pack}}. \quad (12)$$

Our strong binding asymptotics are shown in Fig. 6 along with the MC results of Miller and Frenkel [13].

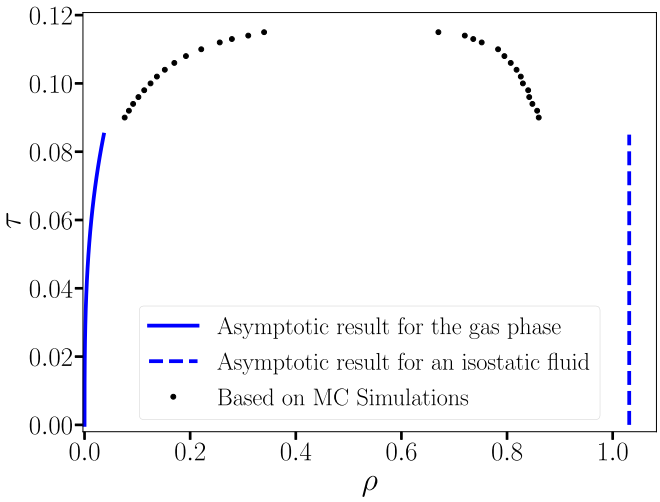

FIG. 6. Strong binding asymptotics applied to the Baxter model derived from our results. The solid blue curve for the gas phase is from Eq. (12), dashed blue line for an isostatic fluid is $\rho = 6\eta_0/\pi$. These results are compared with the coexistence simulation data of Miller and Frenkel from Ref. [13].

VI. CONCLUSION

In summary, we proposed a statistical mechanical description of sphere packings based on treating the coordination number Z as a macroscopic thermodynamic parameter and identified two contributions to the packing entropy: geometric and topological. They correspond to the statistical weight of a particular topological configuration and the number of nonequivalent arrangements, respectively. The topological entropy is thus analogous but not equivalent to Edwards granular entropy or to the residual entropy of hard sphere glasses. An important difference of our approach is that it is built entirely within the framework of equilibrium statistical mechanics and does not impose a requirement on the individual configurations to be jammed. Hence, our results are directly applicable to systems with tensile short-range forces, such as sticky spherical colloids. We developed an MC scheme to compute the geometric and topological entropies of isostatic packings in both 2D and 3D, and further generalized these results for the case of floppy (underconstrained) packings. Finally, we used our results to determine the asymptotic phase behavior of sticky spheres in the limit of strong binding.

ACKNOWLEDGMENTS

The research was carried out at the Center for Functional Nanomaterials, which is a U.S. DOE Office of Science

Facility, at Brookhaven National Laboratory under Contract No. DE-SC0012704.

APPENDIX A: ORIGIN OF FACTOR *N*!

There is considerable confusion in statistical physics literature (including multiple textbooks) regarding the origin of the $N!$ factor that appears in Eq. (1). Traditionally, this factor is introduced as a resolution to the Gibbs paradox, with a justification of the particles (e.g., molecules of a gas) being indistinguishable. It is often claimed that the origin of this factor lies in quantum mechanics. Neither of these justifications is valid. Statistical mechanics of an ideal gas is routinely applied, e.g., to systems of colloids which are neither quantum nor strictly identical. To clarify this issue, consider a system containing N particles that can be exchanged with a much larger system (thermal bath, TB) containing $N_{\rm tot} - N$ particles. All the particles in this example are distinguishable but we assume the free energy of TB to only depend on the total number of particles that it contains, not on their specific subset (e.g., the TB may be an ideal gas). If we start with all particles being in the TB, there are $N_{\rm tot}$ ways of selecting a particle to be moved to the system, then there are $N_{\rm tot} - 1$ ways of selecting the next one, etc. When taking into account the arbitrary order in which N particles can be moved from TB to the system, we obtain the overall statistical weight of the configuration with a given N:

$$\tilde{Z}(N) = \lim_{N_{\rm tot}\to\infty} \frac{N_{\rm tot}!}{N!(N_{\rm tot}-N)!} \frac{Z(N) Z_{\rm TB}(N_{\rm tot}-N)}{Z_{\rm TB}(N_{\rm tot})} = \frac{Z(N) e^{-\mu N}}{N!}. \tag{A1}$$

Here Stirling approximation has been used, yielding $\mu = -\partial \ln(Z_{\rm TB}(N_{\rm tot}))/\partial N_{\rm tot} - \ln N_{\rm tot}$ as the chemical potential of a particle in the TB. The partition function of the system $Z(N)$ is averaged over all possible selections of N particles from $N_{\rm tot}$ that belong to the TB.

APPENDIX B: HIGHER-ORDER CORRECTIONS TO THE ENTROPY

To extrapolate our results from $\lambda = 0$ to $\lambda = 1$, we calculate the response to field λ by using a Landau-style expansion

$$S_{\rm pack} = \lambda S_{\rm geo} + S_{\rm topo} - \frac{s^2}{2\chi} + \frac{s^3}{6\chi'} - \frac{s^4}{24\chi''},$$

where χ, χ', and χ'' represent the product of N with the second, third, and fourth cumulants of $s = S_{\rm geo} - S_{\rm geo}^{(0)}$, respectively.

TABLE II. Entropy values for $\lambda = 1, N = 200$ using a quadratic fit of the response of the entropies to λ, and showing the small corrections when using a quartic fit.

	PBC		Cluster	
	Second order	Fourth order	Second order	Fourth order
$S_{\rm geo}$	0.45	0.40	0.34	0.41
$S_{\rm topo}$	3.12	3.16	2.89	2.85
$S_{\rm pack}$	3.57	3.56	3.23	3.26

The results in Table I have been found to second order and the results in Table II below for $N = 200$ have been expanded to include up to fourth-order terms.

The table shows that higher-order expansions yield only small corrections to the original results.

APPENDIX C: FREE ENERGY OF MASSIVE STICKY SPHERES

We can make contact with previous studies by demonstrating, as others have, that the free energy cannot depend on the moment of inertia or distribution of restoring forces between particles in contact. To do this, we assign arbitrary masses and spring constants to each particle and bond, respectively, and calculate the free energy:

$$Z = \int \prod_i^N \frac{\mathrm{d}^3\mathbf{r}_i \mathrm{d}^3\mathbf{p}_i}{(2\pi\hbar)^d} \exp\left[-\beta \sum_i \left(\frac{\mathbf{p}_i^2}{2m_i} + \sum_{j>i, C_{ij}=1} \frac{k_{ij} x_{ij}^2}{2}\right)\right],$$

$$Z = \frac{|J|}{(2\pi\hbar)^{Nd}} \left[\prod_i^{Nd} (2\pi T m_i)\right]\left[\prod_\alpha^{Nd} \left(\frac{\pi T}{2k_\alpha}\right)\right],$$

$$F = -T \ln Z,$$

$$F = -T\left[\ln(|J|) + Nd \ln\left(\frac{T}{2\hbar}\right) + \frac{1}{2}\ln\left(\prod_i^{Nd} m_i\right) - \frac{1}{2}\ln\left(\prod_\alpha^{Nd} k_\alpha\right)\right].$$

From the free energy, one can see that it only depends on the product of masses and spring constants, despite how they are distributed in the packing. This shows that the free energy, and the entropy, cannot depend on the distribution of masses or restoring forces between particles in contact, and it demonstrates the equivalence between our method of finding the statistical weight of an isostatic packing and the phonon-based method.

[1] T. C. Hales, Historical overview of the kepler conjecture, in *The Kepler Conjecture* (Springer, Berlin, 2011), pp. 65–82.
[2] J. D. Bernal, A geometrical approach to the structure of liquids, Nature (London) **183**, 141 (1959).
[3] S. Torquato, T. M. Truskett, and P. G. Debenedetti, Is Random Close Packing of Spheres Well Defined? Phys. Rev. Lett. **84**, 2064 (2000).
[4] G. Parisi and F. Zamponi, The ideal glass transition of hard spheres, J. Chem. Phys. **123**, 144501 (2005).
[5] S. F. Edwards and R. Oakeshott, Theory of powders, Physica A **157**, 1080 (1989).
[6] S. F. Edwards, The flow of powders and of liquids of high viscosity, J. Phys.: Condens. Matter **2**, SA63 (1990).

[7] G. Parisi and F. Zamponi, Mean-field theory of hard sphere glasses and jamming, Rev. Mod. Phys. **82**, 789 (2010).
[8] C. Song, P. Wang, and H. A. Makse, A phase diagram for jammed matter, Nature (London) **453**, 629 (2008).
[9] C. Briscoe, C. Song, P. Wang, and H. A. Makse, Entropy of Jammed Matter, Phys. Rev. Lett. **101**, 188001 (2008).
[10] D. Asenjo, F. Paillusson, and D. Frenkel, Numerical Calculation of Granular Entropy, Phys. Rev. Lett. **112**, 098002 (2014).
[11] S. Martiniani, K. J. Schrenk, J. D. Stevenson, D. J. Wales, and D. Frenkel, Turning intractable counting into sampling: Computing the configurational entropy of three-dimensional jammed packings, Phys. Rev. E **93**, 012906 (2016).
[12] R. Baxter, Percus-Yevick equation for hard spheres with surface adhesion, J. Chem. Phys. **49**, 2770 (1968).
[13] M. A. Miller and D. Frenkel, Phase diagram of the adhesive hard sphere fluid, J. Chem. Phys. **121**, 535 (2004).
[14] G. Meng, N. Arkus, M. P. Brenner, and V. N. Manoharan, The free-energy landscape of clusters of attractive hard spheres, Science **327**, 560 (2010).
[15] M. Holmes-Cerfon, S. J. Gortler, and M. P. Brenner, A geometrical approach to computing free-energy landscapes from short-ranged potentials, Proc. Natl. Acad. Sci. USA **110**, E5 (2013).
[16] R. W. Perry, M. C. Holmes-Cerfon, M. P. Brenner, and V. N. Manoharan, Two-Dimensional Clusters of Colloidal Spheres: Ground States, Excited States, and Structural Rearrangements, Phys. Rev. Lett. **114**, 228301 (2015).
[17] M. Holmes-Cerfon, Sticky-sphere clusters, Annu. Rev. Condens. Matter Phys. **8**, 77 (2017).
[18] M. E. Cates and V. N. Manoharan, Celebrating soft matter's 10th anniversary: Testing the foundations of classical entropy: Colloid experiments, Soft Matter **11**, 6538 (2015).
[19] E. D. Klein, R. W. Perry, and V. N. Manoharan, Physical interpretation of the partition function for colloidal clusters, Phys. Rev. E **98**, 032608 (2018).
[20] S. Alexander, Amorphous solids: Their structure, lattice dynamics and elasticity, Phys. Rep. **296**, 65 (1998).
[21] A. V. Tkachenko and T. A. Witten, Stress propagation through frictionless granular material, Phys. Rev. E **60**, 687 (1999).
[22] G. Guennebaud, B. Jacob, P. Avery, A. Bachrach, S. Barthelemy, C. Becker, D. Benjamin, C. Berger, A. Berres, J. L. Blanco *et al.*, Eigen v3 (2010), http://eigen.tuxfamily.org
[23] M. P. Ciamarra and A. Coniglio, Random Very Loose Packings, Phys. Rev. Lett. **101**, 128001 (2008).